

Characterization of Methylated Nanoscale MCM-41 Material

X.-D. Li and Q.-Z. Zhai*

Research Center for Nanotechnology, Changchun University of Science and Technology, Changchun 130022, P.R. China

(Received 5 July 2009, Accepted 6 May 2009)

In this study, nanoscale MCM-41 molecular sieve was prepared under a basic condition by a hydrothermal method using cetyltrimethylammonium bromide as a template and tetraethyl orthosilicate as a silica source. Methylated nanoscale MCM-41 molecular sieve was prepared from the nanoscale MCM-41 by post-synthesis method using trimethylchlorosilane (TMCS) as coupling agent. The product was characterized by means of element analysis, powder X-ray diffraction, Fourier transform infrared (FT-IR) spectroscopy, low-temperature nitrogen adsorption-desorption technique at 77 K, scanning electron microscopic (SEM), thermogravimetry-differential thermal analysis (TG-DTA). Powder XRD showed that the framework of the molecular sieve was well retained and the degree of ordering of the methylated MCM-41 decreases. IR spectra and the low-temperature nitrogen adsorption-desorption technique suggested that methyl was successfully grafted to the inner surface of the methylated MCM-41 and the mesoporous channels of the methylated MCM-41 were still maintained. Scanning electron microscopic results showed that the average size of the methylated MCM-41 prepared was 112 nm. Differential thermal analysis showed that the prepared material has preferable thermal stability and the methylated MCM-41 can be stable at 903 °C.

Keywords: Nanoscale MCM-41 molecular sieve, Hydrothermal synthesis, Methylation, Trimethylchlorosilane

INTRODUCTION

Molecular sieves are crystalline aluminosilicate or aluminophosphate materials containing tiny pores of precise and uniform size, which are used as adsorbents, catalyst carriers, desiccants, and so on. Among these materials, ordered mesoporous silicas have received much attention due to their high surface area, well-defined nano-size channels and large pore volume. In 1992, Mobil company developed a new type of mesoporous silica M41S [1,2]. These materials have high internal surface areas, uniform mesoporous aperture and easily controllable pore sizes in the range of 1.6-10 nm. Because of these peculiar characteristics, the synthesis and application of

mesoporous molecular sieves have been investigated by a large number of researchers [3].

MCM-41 is one member of the mesoporous materials family, which contains a hexagonal array of one-dimensional channels of uniform mesopores with a pore diameter of 1.5-10 nm. MCM-41 has attracted the attention of scientists due to its elevated specific surface area, possibility of controlling its pore size and its hydrophobicity and acidity [4,5]. Such special pore architecture makes it a suitable candidate for catalyst [6-9], host-guest chemistry [10-13], biomedicine [14-19], environmental protection [20-24], functional materials with good prospects [25-27], and so on. However, the instability of the structure and the lack of the active center restrict MCM-41 in these ranges of application. Thus a number of studies have been performed in order to find out influence of the synthetic

*Corresponding author. E-mail: zhaiqinzhou@163.com

procedure on mesoporosity, how to improve the thermal and hydrothermal stability [28].

Although the freshly calcined mesoporous silicas consisted mainly of siloxane have hydrophobic surface, the surface becomes hydrophilic because of the easy transformation of siloxane to hydroxyl groups by adsorption of water, the hydrolysis of siloxane may undermine the structure stability of mesoporous silica [29-32]. For example, the ordered mesoporous structure was lost completely on exposure to the air even at room temperature for three months resulting from silicate hydrolysis [29], although both pure-silica and aluminosilicate MCM-41 can be stable at as high as 1123 K in dry or 1073 K in air with low water vapor pressure. The structure of MCM-41 can also be destroyed under mechanical compression due to the mechanochemical hydrolysis of Si-O-Si bonds [30,31].

Fortunately, the thermal stability of mesoporous materials can be improved remarkably by incorporation heteroelements into the silica framework during synthesis procedure or by post-synthetic modification [33,34]. For instance, the introduction of some metal species (such as Al, V) on the surface or into the framework of MCM-41 results in a remarkable improvement of thermal and hydrothermal stability of MCM-41 [35-38]. Yu *et al.* [39] reported that a decrease in surfactant/silicon ratio results in the formation of the mesoporous material with complementary textural porosity which could be useful for improving the structural stability. Chen *et al.* [40] controlled the wall thickness of MCM-41 by increasing crystallization time to 1 ~ 7 days at 165 °C at mild basic conditions. The remarkable hydrothermal stability of MCM-41 synthesized in this study was demonstrated. Zelenak *et al.* [41] investigated the thermal stability of mesoporous silica modified with titania in the range of temperature from 923 to 1273 K. Galacho *et al.* [42] evaluated the thermal stability of Ti-MCM-41 in air towards heating up to 1373 K and prepared the Ti-MCM-41 with different metal content and two different surfactants.

The structural stability of mesoporous molecular sieves organically functionalised by a direct method and a comparison with the purely inorganic MCM-41 has also been a subject of investigation by Inagaki *et al.* [3]. In addition, Luechinger *et al.* [43] focused on the effects of different procedures for adding acetic acid during the synthesis of

MCM-41 and the hydrothermal stability of pure silica MCM-41.

Nanoscale MCM-41 molecular sieves was prepared by Cai *et al.* in 2001 [44]. MCM-41 has a lower mechanical strength [45] and a lower hydrothermal stability [46] than zeolites. By post-modification, the surface silanols serve as reactive sites and can be replaced by organic groups. Therefore, it is expected that for the methylated MCM-41, the thermal stability can be effectively improved compared with the conventional pure silica MCM-41. In this paper, we report the preparation method of methylated nanoscale MCM-41 materials and its characterization using the element analysis, power X-ray diffraction, FT-IR, low temperature nitrogen adsorption-desorption study at 77 K, SEM and TG-DTA analysis. The effectiveness of methylated MCM-41 was studied; the thermal stability of the methylated MCM-41 was enhanced compared with that of the unmodified MCM-41.

EXPERIMENTAL

Reagents

The following reagents were used: tetraethyl orthosilicate (TEOS, Sinopharm Chemical Reagent Co., Ltd., China); cetyltrimethylammonium bromide (CTMAB, Changzhou Xinhua Research Institute for Reagent, China); sodium hydroxide (Beijing Chemical Reagent Plant, China); trimethylchlorosilane (TMSCl, Sinopharm Chemical Reagent Co., Ltd., China); benzene (Tianjin Guangfu Fine Chemical Research Institute, China); absolute ethanol (Beijing Chemical Reagent Plant, China); deionized water.

Preparation of Methylated MCM-41 by Post-Synthesis Method

The host nanoscale MCM-41 molecular sieve was prepared by a hydrothermal method using tetrathyl orthosilicate as a silica source and CTMAB as a structure-directing agent. A 1.0 g of CTMAB was added into 480 ml of deionized water at 80 °C under vigorous stirring. When the solution became homogeneous, 3.5 ml of 2 M NaOH solution was added with stirring. After the solution became homogeneous, 5.0 ml of TEOS was slowly dropped, giving rise to a white slurry. Then the reaction mixture was kept at 80 °C for 2 h with stirring. The resulting solid was recovered by

Characterization of Methylated Nanoscale MCM-41 Material

filtration, extensively washed with deionized water, and dried at ambient temperature. The template was removed by calcination at 500 °C for 4 h. The unmodified MCM-41 molecular sieve was obtained, and the size of the prepared material was calculated to be 111 nm from SEM images (see Fig. 6A). 0.8039 g of the unmodified MCM-41 was added into the mixed solution which was made up of 10 ml of benzene and 8 ml of trimethylchlorosilane at the room temperature of 20 °C with stirring for 72 h. Then, the resulting product was filtrated and washed twice with absolute ethanol. Finally, the prepared material was dried at 300 °C for 6 h, and the prepared product was the methylated nanoscale MCM-41.

Apparatus

Elemental analysis was performed by elementary organic microanalysis for C and H in a VERIOEL element analyzer. The content of Si was determined by siliconantimomolybdate heteropoly blue photometry [47]. The powder X-ray diffraction (XRD) patterns were recorded using a Siemens D5005 X-ray diffractometer (Germany), where a Cu K α target ($\lambda = 0.15418$ nm and operating at 30 kV and 20 mA) was used as the X-ray source. Data were collected between the 2θ range of 0.4 – 10° with a resolution of 0.02° . Infrared spectra were recorded on the American Nicolet 5DX-FTIR spectrometer with potassium bromide pellets. Low temperature nitrogen adsorption and desorption isotherms were measured at 77 K on a Micromeritics ASAP 2010M system (The American Mike Company). The data were calculated in terms of the model of Broekhoff and de Boer (BdB) [48]. Surface area and pore volume were calculated by following BET [49] and BJH [50] procedures, respectively. Scanning electron microscopy (SEM) images were taken on a PHILIPS XL30 SEM instrument. The TG-DTA curves were obtained using a Perkin Elmer SDT2960 thermogravimetric analyzer in the temperature range of 20–1000 °C under dynamic nitrogen atmosphere (100 ml min^{-1}) and heating rate of 10 °C min^{-1} .

RESULTS AND DISCUSSION

Element Analysis

The content of C and H elements in the methylated MCM-41 sample was determined with the element analyzer. The content of Si in the methylated MCM-41 was determined by

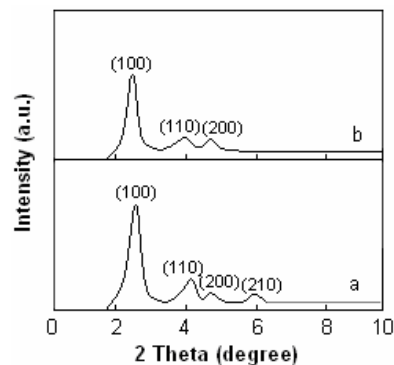


Fig. 1. XRD patterns of the samples: (a) unmodified MCM-41; (b) methylated MCM-41.

molybdsilicate blue photometry [47]. The contents of C, H, Si and O obtained were 8.86%, 1.15%, 22.15% and 67.84% in weight, respectively. Thus the molecular formula of the prepared material calculated was $\text{C}_{7.4}\text{H}_{34.5}\text{Si}_{7.9}\text{O}_{42.4}$.

Powder XRD Analysis

Figure 1 shows that the powder X-ray diffraction patterns of the unmodified MCM-41 molecular sieve and the methylated MCM-41 materials. The XRD patterns of these materials show typical characteristic four-peaks with very strong one at a low 2θ and three (unmodified MCM-41) or two (methylated MCM-41) weak peaks at higher 2θ values, and it can be indexed according to the hexagonal unit cell [44]. The methylated MCM-41 has three diffraction peaks that can be indexed as (100), (110) and (200), respectively. Meanwhile, the diffraction peak of (210) of the methylated MCM-41 disappeared, suggesting that the order degree of the methylated MCM-41 has reduced. The diffraction intensity of the methylated MCM-41 decreases compared with that of the unmodified MCM-41, indicating that the crystallinity of the methylated MCM-41 has decreased.

FT-IR Spectra Analysis

Figure 2 shows the FT-IR spectra of the unmodified MCM-41 and methylated MCM-41 samples. The peaks at 3512 and 960 cm^{-1} , which are assigned to O-H and Si-O stretching of the surface silanols of the unmodified MCM-41, respectively, almost disappeared for the methylated MCM-41. The peak of

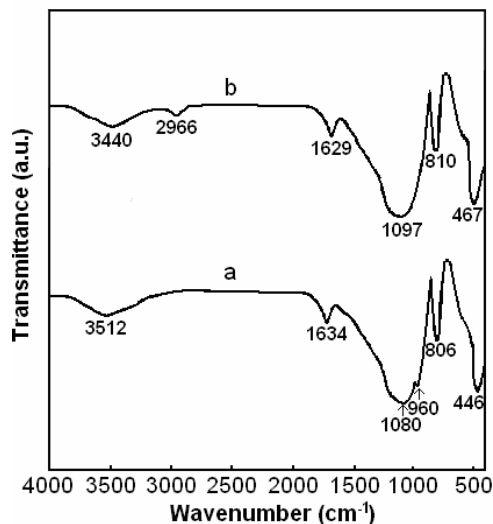


Fig. 2. Infrared spectra of the samples: (a) unmodified MCM-41; (b) methylated MCM-41.

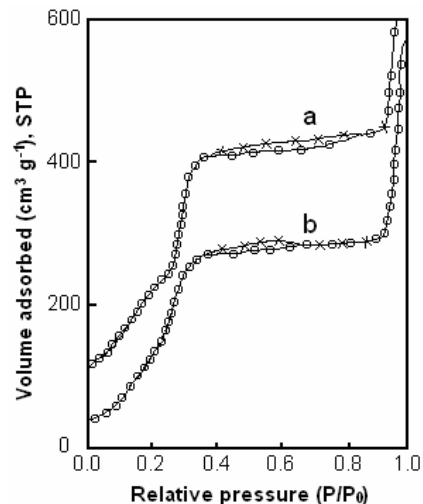


Fig. 4. Low temperature nitrogen adsorption-desorption isotherms (\circ adsorption, \times desorption). (a) unmodified MCM-41, (b) methylated MCM-41.

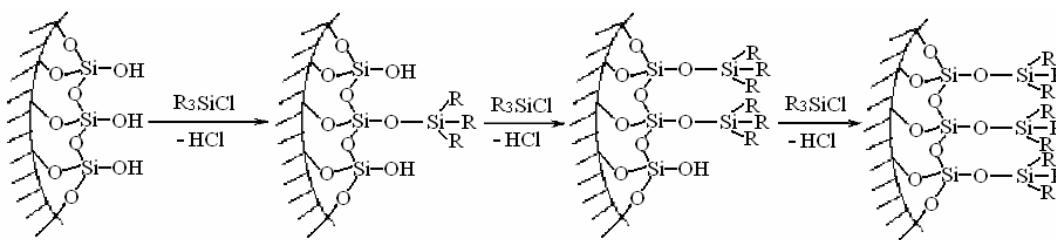


Fig. 3. Chemical reaction of trimethylchlorosilane and unmodified MCM-41, $R = -CH_3$.

the unmodified MCM-41 at 1080 cm^{-1} can be attributed to the asymmetric stretching vibration of the Si-O-Si band and 806 cm^{-1} can be assigned to the symmetric stretching vibration of Si-O. For the methylated MCM-41, the peak at 3512 cm^{-1} of the symmetric stretching vibration shifted towards lower wavenumber. The peak at 960 cm^{-1} assigned to Si-OH disappeared for the methylated sample because the silanol was replaced by Si-CH₃ as Fig. 3. The presence of a stretching band at 2966 cm^{-1} in the methylated MCM-41 sample shows the presence of methyl in the framework.

Low Temperature Nitrogen Adsorption-Desorption Isotherms and Pore Size Distribution

The N₂ adsorption-desorption isotherms and the BJH pore

size distribution of the unmodified MCM-41 and methylated MCM-41 are shown in Figs. 4 and 5. They all exhibit type IV isotherms with H1-type hysteresis loops at low relative pressure, which is related to the capillary condensation of nitrogen within the pores. According to IUPAC classification [51], they are features of typical of mesoporous structure solids, indicating that the mesoporous structure was still maintained after methylation. From the two branches of adsorption-desorption isotherms, the presence of a sharp adsorption step in the P/P_0 region 0.2 to 0.4 shows that all samples possess well-defined arrays of regular mesopores. However, the relative pressure where capillary condensation occurred shifted to lower position and the pore diameter was decreased. The specific area and the pore size were calculated

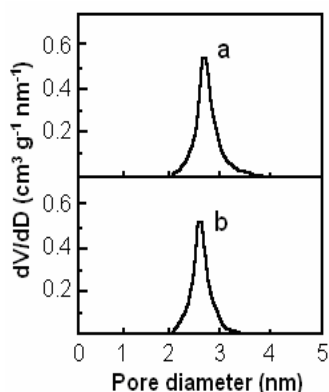


Fig. 5. Pore size distribution patterns of the samples: (a) unmodified MCM-41, (b) methylated MCM-41.

by the BET method and BJH model, respectively. Samples display a narrow pore size distribution. The surface area, pore volume and effective pore diameters of the samples are summarized in Table 1. It can be clearly seen that the BET surface area of methylated MCM-41 is $920.60 \text{ m}^2 \text{ g}^{-1}$ and decreases $40.30 \text{ m}^2 \text{ g}^{-1}$ compared with that of the unmodified MCM-41, and the average pore diameter and pore volume also decreased from 2.29 nm and 0.566 ml g^{-1} to 2.08 nm and 0.528 ml g^{-1} , respectively. All these results together with the increased thickness of pore walls can be attributed to the replacement of silanol groups on the inner surface by methyl. The stability of methylated nanoscale MCM-41 material will be further enhanced when the surface silanol groups are linked together by organic groups [52-55].

Table 1. Pore Structure Parameters of the Samples

Sample	Crystal face spacing/ $d_{(100)}$ (Å) ^a	Unit cell parameter/ a_0 (Å) ^b	BET surface area ($\text{m}^2 \text{ g}^{-1}$)	Specific pore volume (ml g^{-1}) ^c	Pore size (Å) ^d	Wall thickness (Å) ^e
Unmodified MCM-41	33.4	38.5	960.90	0.566	22.9	15.6
Methylated MCM-41	33.8	39.0	920.60	0.528	20.8	18.2

^a d_{100} is crystal face spacing obtained from XRD pattern. ^b a_0 is unit cell parameter, the repeat distance between two pore centers in MCM-41 molecular sieve; $a_0 = \frac{2}{\sqrt{3}} d_{100}$. ^cPore volume is BJH adsorption cumulative volume of pores. ^dPore size is calculated

from the adsorption branch. ^eWall thickness is calculated by (a_0 - pore size).

SEM Analysis

Figure 6 show the representative SEM images of the unmodified MCM-41 and methylated MCM-41 samples. In Fig. 6A, small spherical particles of unmodified MCM-41 are evident. It can be clearly seen that the nanoparticles stack compactly and particle interstices with nominal diameter averaging 111 nm are consistently found [44]. The SEM image of methylated MCM-41 (Fig. 6B) showed regular spherical type morphology which is rather similar to that of the unmodified MCM-41, however, the ball particles can be consistently seen, and the average size of the particle was 112 nm .

TG-DTA Analysis

Figure 7 shows the results of DTA-TG for the unmodified MCM-41 and methylated MCM-41 samples. From Fig. 7A, the DTA curve for unmodified MCM-41 show significantly endothermic peak from 52 to $110 \text{ }^\circ\text{C}$, which indicates the thermodesorption of physically adsorbed water. The other endothermic peak appears at approximately $314 \text{ }^\circ\text{C}$, which corresponds to the residual surfactant decomposition and silanol condensation. Furthermore, the evidently endothermic peak with a maximum at $854 \text{ }^\circ\text{C}$ appears, which indicates the collapses of mesoporous structure of the unmodified MCM-41. Comparing Fig. 7B with 7A, the result of the TG analysis indicates 0.460% weight loss of the composite at $100 \text{ }^\circ\text{C}$ corresponding to the endothermic peak of the DTA curve at $100 \text{ }^\circ\text{C}$, resulting from the exterior physically adsorbed water. With the temperature rise, the other endothermic peak of the

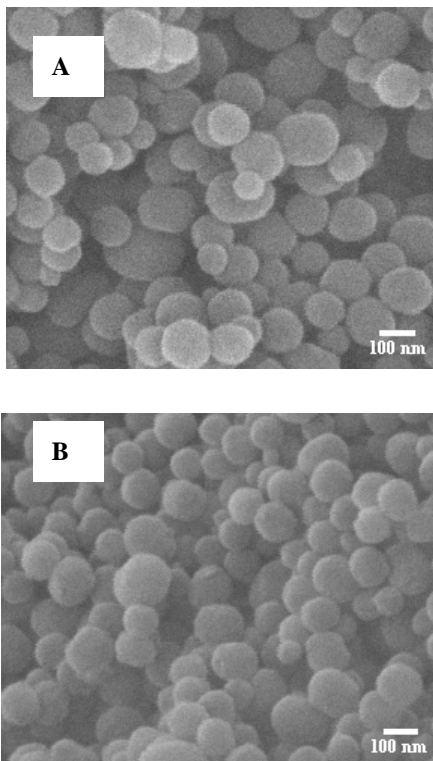


Fig. 6. Scanning electron micrographs of samples: (A) unmodified MCM-41, (B) methylated MCM-41.

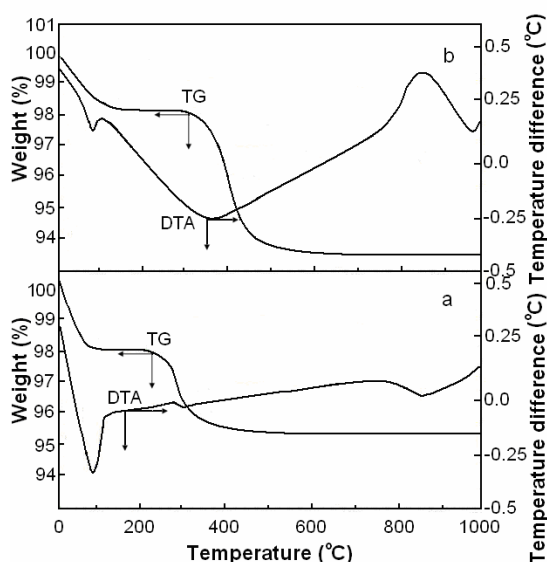


Fig. 7. DTA-TG patterns of samples: (A) unmodified MCM-41, (B) methylated MCM-41.

DTA curve appears at 375 °C due to the hydroxyl dehydration of molecular sieves with a weight loss of 1.53%. Over the range of 404-881 °C, the DTA curve shows 4.17% weight loss of the composite resulting from the oxidation of surface methyl, which gives rise to the thermal release and DTA profile with an exothermic peak at 852 °C. The weight did not change between 881 and 1000 °C. It is observed in the DTA curve that the endothermic peak at 903 °C can be assigned to the collapses of framework of the sample. Unmodified MCM-41 can be stable up to 850 °C in dry air [56]. It is interesting that the methylated MCM-41 exhibits an excellent and better thermal stability compared with the unmodified MCM-41.

CONCLUSIONS

Methylated nanoscale MCM-41 molecular sieve has been successfully prepared and a series of characterization techniques have demonstrated that methyl has been grafted to the MCM-41 and the thermal stability of MCM-41 can be significantly improved. Elemental analysis, powder XRD, IR spectroscopy, low temperature N₂ adsorption-desorption, SEM and TG-DTA were adopted to characterize the methylated MCM-41. The results showed that a methyl group has been successfully grafted to the nanoscale MCM-41 molecular sieve, and the methylated MCM-41 still retains the structure of the MCM-41. The adsorption technique further indicated that methyl grafted to the inner surface of the nanoscale MCM-41. SEM results indicated that the average size of the methylated MCM-41 was 112 nm. TG-DTA results revealed that the prepared material has better thermal stability compared with the unmodified MCM-41.

REFERENCES

- [1] C.T. Kresge, M.E. Leonowicz, W.J. Roth, J.C. Vartuli, J.S. Beck, *Nature* 359 (1992) 710.
- [2] J.S. Beck, J.C. Vartuli, W.J. Roth, M.E. Leonowicz, C.T. Kresge, K.D. Schmitt, C.T. Chu, D.H. Olson, E.W. Sheppard, S.B. McCullen, J.B. Higgins, J.L. Schienker, *J. Am. Chem. Soc.* 114 (1992) 10834.
- [3] N. Igarashi, K. Hashimoto, T. Tatsumi, *J. Mater. Chem.* 12 (2002) 3631.

Characterization of Methylated Nanoscale MCM-41 Material

- [4] R.A.A. Melo, M.V. Giotto, J. Rocha, E.A. Urquieta-Gonzalez, *J. Mater. Res.* 2 (1999) 173.
- [5] U. Ciesla, F. Schuth, *Micropor. Mesopor. Mater.* 27 (1999) 131.
- [6] A. Corma, *Chem. Rev.* 97 (1997) 2373.
- [7] D.E. De Vos, M. Dams, B.F. Sels, P.A. Jacobs, *Chem. Rev.* 102 (2002) 3615.
- [8] A.P. Wight, M.E. Davis, *Chem. Rev.* 102 (2002) 3589.
- [9] M. Guidotti, I. Batonneau-Gener, E. Gianotti, L. Marchese, S. Mignard, R. Psaro, M. Sgobba, N. Ravasio, *Micropor. Mesopor. Mater.* 111 (2008) 39.
- [10] K. Moller, T. Bein, *Chem. Mater.* 10 (1998) 2950.
- [11] N.K. Mal, M. Fujiwara, Y. Tanaka, *Nature* 421 (2003) 350.
- [12] Y. Wan, H.F. Yang, D.Y. Zhao, *Acc. Chem. Res.* 39 (2006) 423.
- [13] Q.Z. Zhai, Y.X. Liu, *Chin. J. Chem. Phys.* 20 (2007) 83.
- [14] M. Vallet-Regi, A. Ramila, R.P. Del Real, J. Perez-Pariente, *Chem. Mater.* 13 (2001) 308.
- [15] B. Munoz, A. Ramila, J. Perez-Pariente, I. Diaz, M. Vallet-Regi, *Chem. Mater.* 15 (2003) 500.
- [16] J. Andersson, J. Rosenholm, S. Areva, M. Linden, *Chem. Mater.* 16 (2004) 4160.
- [17] W.C. Nigel, L.K. Swaminathan, C.L. Raston, *J. Mater. Chem.* 18 (2008) 162.
- [18] Y.Z. You, K.K. Kalebaila, S.L. Brock, D. Oupicky, *Chem. Mater.* 20 (2008) 3354.
- [19] S.B. Wang, *Micropor. Mesopor. Mater.* 117 (2009) 1.
- [20] R.I. Nooney, M. Kalyanaraman, G. Kennedy, E.J. Maginn, *Langmuir* 17 (2001) 528.
- [21] A. Sayari, S. Hamoudi, Y. Yang, *Chem. Mater.* 17 (2005) 212.
- [22] D. Perez-Quintanilla, I. Del Hierro, M. Fajardo, I. Sierra, *J. Mater. Chem.* 16 (2006) 1757
- [23] X.M. Xue, F.T. Li, *Micropor. Mesopor. Mater.* 116 (2008) 116.
- [24] K. Dimos, P. Stathi, M.A. Karakassides, Y. Deligiannakis, *Micropor. Mesopor. Mater.* 126 (2009) 65.
- [25] J.L. Shi, Z.L. Hua, L.X. Zhang, *J. Mater. Chem.* 14 (2004) 795.
- [26] S. Tangestaninejad, M. Moghadam, V. Mirkhani, I. Mohammadpoor-Baltork, K. Ghani, *J. Iran. Chem. Soc.* 5 (2008) S71.
- [27] M. Pal, V. Ganesan, *Langmuir* 25 (2009) 13264.
- [28] A. Davidson, *Curr. Opin. Colloid Interface Sci.* 7 (2002) 92.
- [29] X.S. Zhao, F. Audsley, G.Q. Lu, *J. Phys. Chem. B* 102 (1998) 4143.
- [30] T. Tatsumi, K.A. Koyano, Y. Tanaka, S. Nakata, *J. Porous. Mater.* 6 (1999) 13.
- [31] A. Matsumoto, T. Sasaki, N. Nishimiya, K. Tsutsumi, *Langmuir* 17 (2001) 47.
- [32] K. Cassiers, T. Linssen, M. Mathieu, M. Benjelloun, K. Schrijnemakers, P. Van Der Voort, P. Cool, E.F. Vansant, *Chem. Mater.* 14 (2002) 2317.
- [33] A. Tuel, *Micropor. Mesopor. Mater.* 27 (1999) 151.
- [34] Q.G. Meng, P. Boutinaud, A.C. Franville, H.J. Zhang, R. Mahiou, *Micropor. Mesopor. Mater.* 65 (2003) 127.
- [35] R. Mokaya, W. Jones, *J. Mater. Chem.* 9 (1999) 555.
- [36] S.C. Shen, S. Kawi, *J. Phys. Chem. B* 103 (1999) 8870.
- [37] S.C. Shen, S. Kawi, *Langmuir* 18 (2002) 4720.
- [38] J.Q. Xu, W. Chu, S.Z. Luo, *J. Mol. Catal. A: Chem.* 256 (2006) 48.
- [39] J. Yu, J.L. Shi, L.Z. Wang, M.L. Ruan, D.S. Yan, *J. Mater. Sci. Lett.* 20 (2001) 289.
- [40] C.F. Cheng, S.H. Chou, P.W. Cheng, H.H. Cheng, H.K. Yak, *J. Chin. Chem. Soc.* 54 (2007) 35.
- [41] V. Zelenak, V. Hornebecq, S. Mornet, O. Schaf, P. Llewellyn, *Chem. Mater.* 18 (2006) 3184.
- [42] C. Galacho, M.M.L. Ribeiro Carrott, P.J.M. Carrott, *Micropor. Mesopor. Mater.* 108 (2008) 283.
- [43] M. Luechinger, L. Frunz, G.D. Pirngruber, R. Prins, *Micropor. Mesopor. Mater.* 64 (2003) 203.
- [44] Q. Cai, Z.S. Luo, W.Q. Pang, Y.W. Fan, X.H. Chen, F.Z. Cui, *Chem. Mater.* 13 (2001) 258.
- [45] D.D. Giscard, O. Collart, A. Galameau, P. Van Der Voort, F.D. Renzo, F. Fajula, *Stud. Surf. Sci. Catal.* 129 (2000) 665.
- [46] K.A. Koyano, T. Tatsumi, *J. Phys. Chem. B* 101 (1997) 9436.
- [47] Q.Z. Zhai, Y.C. Kim, *Chin. J. Spectrosc. Lab.* 15 (1998) 82.
- [48] J.C.P. Broekhoff, J.H. Deboer, *J. Catal.* 10 (1968) 307.
- [49] S. Brumauer, P.H. Emmett, E. Teller, *J. Am. Chem. Soc.* 60 (1938) 309.

- [50] E.P. Barrett, L.G. Joyner, P.P. Halenda, *J. Am. Chem. Soc.* 73 (1951) 373.
- [51] K.S.W. Sing, D.H. Everett, R.A.W. Haul, L. Moscou, R.A. Pierotti, J. Rouquerol, T. Siemieniewska, *Pure. Appl. Chem.* 57 (1985) 603.
- [52] X.S. Zhao, G.Q. Lu, *J. Phys. Chem. B* 102 (1998) 1556.
- [53] X.S. Zhao, G.Q. Lu, X. Hu, *Micropor. Mesopor. Mater.* 41 (2000) 37.
- [54] B. Lindlar, M. Luchinger, A. Rothlisberger, M. Haouas, G. Pirngruber, A. Kogelbauer, R. Prins, *J. Mater. Chem.* 12 (2002) 528.
- [55] R.R. Sever, R. Alcalá, J.A. Dumesic, T.W. Root, *Micropor. Mesopor. Mater.* 66 (2003) 53.
- [56] C.Y. Chen, H.X. Li, M.E. Davis, *Micropor. Mater.* 2 (1993) 17.